Brain White Matter Network Analysis of Autism Spectrum Disorder - CS224W Project Milestone

Anton Apostolatos
Computer Science Department
Stanford University
antonaf@cs.stanford.edu

1 Introduction

In this paper we will be examining and analyzing the white matter structure of pre-teens and adolescent individuals with autism spectrum disorder (ASD) as collected through diffusion tensor imaging and developed with tractography. Given the pivotal nature of axon tracts on coordinating communication among brain regions (Fields, 2008), and the inherent network-like structure of these tracts, we believe that network and graph analysis may provide greater insight and understanding on the relationship between ASD and white matter structure.

More specifically, we will be examining the neural networks of 52 subjects with ASD and 43 under typical development (TD) as unique, weighted, undirected graphs, with nodes being brain regions and edges being the existence and number of neural connections between these regions. Our initial focus is on understanding various features of these regions and their interconnections, including centrality, clustering and motif analysis. In order to ground our analysis, we will be using the non-parametric Friedman test and the Wilcoxon rank-sum test to highlight any statistically significant differences between the two subject groups, tying our results back to current medical knowledge on the relationship between ASD and white matter structure in the brain.

2 Related Work

2.1 DTI and Autism

Diffusion tensor imaging (DTI) tractography is a technique used to represent white-matter neural tracts in the brain – namely, axon tracts and commissures. White matter has an active effect on learning, self-control, and mental illness, controlling the signals that neurons share (Fields, 2008).

Autism spectrum disorder (ASD) is a group of neurodevelopmental disorders with characteristics that include impaired social cognition and reciprocity, and repetitive, restricted behavior (NIMH, 2016; Lord et al., 2000).

There is evidence that a connection between ASD and abnormal white matter structure exists with studies on children and adolescents with autism finding that disruption of white matter tracts in white matter adjacent to the ventromedial prefrontal cortices, in the anterior cingulate gyri and the temporopatietal junctions may be implicated in impaired social cognition for individuals with with ASD (Barnea-Goraly et al., 2004). Developmental studies of white matter in males suffering from ASD has found that there is a reduction in the structural integrity of white matter – namely, lower fractional anistrophy near the corpus callosum and in the right retrolenticular portion of the internal capsul – that may underlie the behavioral pattern observed in autism (Keller et al., 2007). Recent studies have been placing more attention on analyzing how the nature of abnormality in white matter integrity affects ASD behavioral phenomena, though most work has been kept within the boundaries of biological analysis of white matter fiber tracts (Pryweller et al., 2014; ACE, 2016). We believe that representing white matter structure as a graph and using complex network methods and measures to analyze information gather with DTI scans may help us gain further insight as to how ASD is associated with white matter formation and structure in the brain.

2.2 Brain Neural Network Analysis

The network structure of brain connectivity is a popular topic of research and exploration. The uses and interpretations of a wide array of network measures and tools have been well documented, including measures of segregation and integration, centrality, and resilience (Rubinov and Sporns, 2010). Various mapping techniques, including functional magnetic resonance imaging,

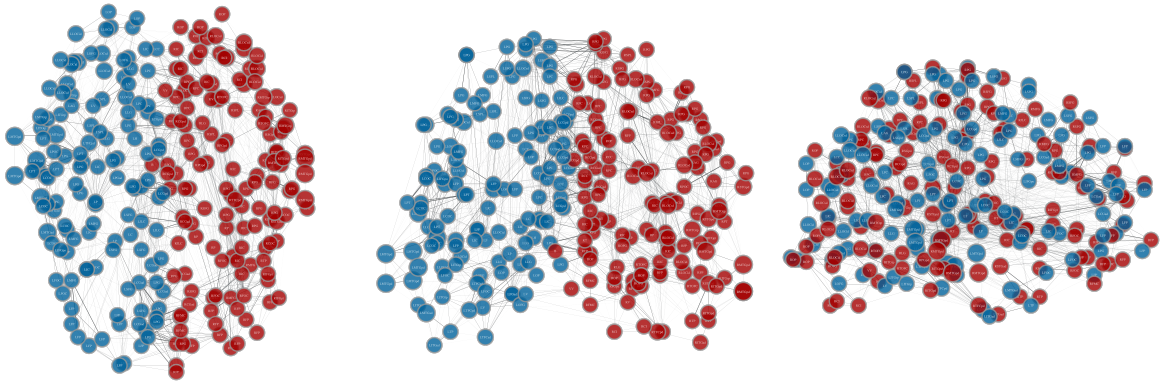

(a) Horizontal plane (b) Coronal plane (c) Sagittal plane

Figure 1: ASD white matter structure from DTI tractography

electroencephalogram, magnetoencephalography, and susceptibility tensor imaging, which capture different aspects of the functional or anatomical structure of the brain, have been analyzed with various network tools and methods (Sporns et al., 2007; Joyce et al., 2010). For instance, eigenvector centrality has been used for analyzing connectivity patterns in temporal fMRI data of the brain, with the authors concluding that the tool is an effective and computationally efficient tool for capturing intrinsic neural architecture at a voxel-wise level (Lohmann et al., 2010).

An effort to evaluate the brain architecture in autism does exist, with the Autism Imaging Data Exchange consortium aggregating and sharing over a thousand resting-state fMRI datasets of male subjects with ASD and TD (Di Martino et al., 2014). However, the structural information captured by fMRI scans is very different to that collected in DTI tractography methods – namely, while DTI tractography attempts to reveal the white matter structure of the brain, fMRI measures brain activity through changes in blood flow (Matthews and Jezzard, 2004). Notably, little work has been done in analyzing and comparing the white matter structure of the brain of individuals with ASD, despite the strong belief that myelination and white matter development in infant and teenage years can be different for people with ASD.

3 Data

We will be working with diffusion tensor imaging (DTI) data collected by the Center for Autism Research and Treatment at UCLA, obtained from the USC Multimodal Conenctivity Database (Brown et al., 2012). The sample consists of 52 subjects with autism spectrum disorders (ASD) and 43 individuals under typical development (TP), all between the ages of 8 and 18. These two groups do not have statistically significant differences in their sex, age, mean and maximum head motion, or their full-scale, verbal, and performance IQ (Rudie et al., 2013). The data was collected on a Siemens 3T Trio scanning device at UCLA. After being asked to relax and keep their gaze focused on a fixation cross on a screen, T2*-weighted functional images were captured, with a TR of 3000ms, TE of 27ms, a 128×128 matrix size, 192mm FoV and 3.0×3.0mm in-plane voxel dimensions. These scans were consequently analyzed and preprocessed, with individuals with excessive motion not included in the final dataset (Rudie et al., 2013). Brain deterministic tractography, which aims to represent the neural tracts collected by the diffusion MRI images, was then preformed on the scans using the Fiber Assignment by Continuous Tracking (FACT) algorithm (Mori and van Zijl, 2002), a state of the art method for fiber tracking from DTI imaging data. Fibers shorter than three voxels were discarded (no turn angle can be determined from just two voxels). The maximum turn angle of fibers propagating from voxels was of 50^o (Zalesky et al., 2010). Fibers were consequently smoothed using spline filters (Rudie et al., 2013).

The final data consists of 264 putative functional areas as defined by (Power et al., 2011), where edges between these regions correspond to the number of fibers where one endpoint finished in one region and the other endpoint in the other (Rudie et al., 2013). The data was structured in a

264×264 whole brain structural connectivity matrix. Each of the 94 subjects has a corresponding connectivity matrix. Figure 1 shows the graph for one of the individuals with ASD.

4 Methods

We will survey the various tools and measures we are going to be using to analyze the graphs, as well as the statistical methods we are going to be using to evaluate the statistical significance of the differences captured by these models on the two subject groups. Some of these measures are on an entire graph, while others capture information on a per-vertex basis.

4.1 Clustering

Clustering of brain networks attempts to capture the interconnectivity of groups or clusters within the network. The organization of dependencies captured by these methods may indicate the existence of segregated neural processing (Rubinov and Sporns, 2010). We will be calculating the local clustering coefficient of every node in every graph. This coefficient c is for node n is defined as

$$c_n = \frac{t_n}{k_n(k_n - 1)}$$

where t_n is the number of triangles around a node n and k_n is the degree of node n. We will also be calculating the global clustering coefficient, defined as the average of the clustering coefficients of each node.

4.2 Transitivity

An issue with the clustering coefficient is that it may be disproportionately influenced by nodes with low degrees (Rubinov and Sporns, 2010). The transitivity does not suffer from this problem, and is defined as follows

$$T = \frac{\sum_{n \in N} 2t_n}{\sum_{n \in N} k_n(k_n - 1)}$$

4.3 Centrality

We'll be using a number of measures to calculate the centrality of the brain region nodes of our graphs. Each of these centrality measures captures different nuances about the importance and influence of various nodes in our graphs. We proceed with short introductions of the various centrality measures utilized in this project.

4.3.1 Closeness Centrality

The closeness c of any given vertex n_i is defined as

$$c_n = \frac{1}{\sum_{n_j} w_{n_i,n_j}}$$

where w_{n_i,n_j} is the weight of the edge between nodes n_i and n_j (Opsahl et al., 2010).

4.3.2 Betweenness Centrality

We define the betweenness centrality of a node n as

$$c(n) = \sum_{n_i \neq n_j \neq n} \frac{\sigma_{n_i,n_j}(n)}{\sigma_{n_i,n_j}}$$

where σ_{n_i,n_j} is the number of shortest paths between n_i and n_j, and $\sigma_{n_i,n_j}(n)$ the number of shortest paths between n_i and n_j that pass through n (Brandes, 2001).

4.3.3 Eigenvector Centrality

The eigenvector centrality $\mathbf{x}$ of a list of vectors $\mathbf{n}$ with weighted adjacency matrix $\mathbf{A}$ is defined as the eigenvector with the largest eigenvalue λ (Langville and Meyer, 2005). Namely, it is the solution of $\mathbf{Ax} = \lambda\mathbf{x}$ where λ is the largest eigenvalue.

4.3.4 Authority and Hubs

Authorities $\mathbf{y}$ and hubs $\mathbf{x}$ are defined as

$$\mathbf{x} = \alpha\mathbf{A}\mathbf{y}$$

$$\mathbf{y} = \beta\mathbf{A}^\top\mathbf{x}$$

where $\mathbf{A}$ is the weighted adjacency matrix and $\lambda = (\alpha\beta)^{-1}$ is the largest eigenvalue of $\mathbf{A}\mathbf{A}^\top$ (Kleinberg, 1999). Since our graphs are undirected, then our adjacency matrix is symmetric along the diagonal. Thus, λ will be the singular value of $\mathbf{A}$ and $\mathbf{x} = \mathbf{y}$. Therefore, the authority and hub value for every node will be the same (we will be reporting a single value for each node).

4.3.5 PageRank

For any node n the PageRank value $R(n)$ is defined iteratively by

$$R(n) = \left(\frac{1-d}{N}\right) + d \sum_{x \in \Gamma(n)} \frac{R(x)A_{n,x}}{\sum_y A_{n,y}}$$

where A is a weighted adjacency matrix, $\Gamma(n)$ are the neighbors of n, and d is a damping factor (Page et al., 1999).

Clustering	Closeness	Betweenness	PageRank	Eigenvector	Authority
ROP : 0.6452	B : 0.3193	B : 0.0481	B : 0.0067	RSFG : 0.1335	RSFG : 0.1335
LCOC : 0.6245	LT : 0.3042	LP : 0.0358	LPT : 0.0065	RPG : 0.1204	RPG : 0.1204
LFP : 0.5889	RPGpd : 0.3036	RT : 0.0296	RFOC : 0.0061	B : 0.0944	B : 0.0944
RMTGp : 0.5853	RT : 0.3023	RPGpd : 0.0296	RSFG : 0.0051	RCGad : 0.0818	RCGad : 0.0818
LPOC : 0.5683	LH : 0.3013	LT : 0.0295	RPOC : 0.0051	LJLC : 0.0814	LJLC : 0.0814

Table 1: Top nodes and average corresponding values for various metrics for TD subjects

Clustering	Closeness	Betweenness	PageRank	Eigenvector	Authority
ROP : 0.6721	B : 0.3169	B : 0.0474	B : 0.0066	RPG : 0.1396	RPG : 0.1396
LFP : 0.6504	RT : 0.2998	RP : 0.0318	LPT : 0.0064	RSFG : 0.1379	RSFG : 0.1379
LCOC : 0.6387	RP : 0.2985	RT : 0.0275	RFOC : 0.0061	B : 0.1163	B : 0.1163
RAG : 0.5908	LH : 0.2984	LP : 0.0266	RCGpd : 0.0051	RCGad : 0.0963	RCGad : 0.0963
RMTGp : 0.5782	LT : 0.2952	LH : 0.0259	RPOC : 0.0050	LJLC : 0.0949	LJLC : 0.0949

Table 2: Top nodes and average corresponding values for various metrics for ASD subjects

4.4 Characteristic Path Length

The characteristic path length L is defined as the mean averaged distance between every node and every other node. Namely

$$L = \frac{1}{n}\sum_{i \in N} L_i = \frac{1}{n}\sum_{i \in N} \frac{\sum_{j \in N, j \neq i} d_{ij}}{n-1}$$

where $d_i j$ is the length of the shortest path between nodes i and j, where, if no path exists, $d_{ij} = \infty$ (Rubinov and Sporns, 2010).

4.5 Efficiency

The efficiency of a graph is a measure of how well and efficiently information can be transmitted across the network (Rubinov and Sporns, 2010). The efficiency E_i of a node i is defined as

$$E_i = \frac{\sum_{j \in N, j \neq i} {d_{ij}}^{-1}}{n-1}$$

The efficiency has been argued to be a more meaningful measure of integration than shortest path length since rather than being influenced by long paths it's influenced primarily by short paths (Achard and Bullmore, 2007). The global efficiency of a network is the average efficiency of all of its nodes, as follows:

$$E = \frac{1}{n}\sum_{i \in N} E_i$$

4.6 Statistical Tests

We will be using two statistical tests to capture the statistical significance between any differences found between the two subject pools. The Friedman non-parametric test will be used on metrics that are captures on a per-node basis, while the Wilcoxon signed-rank test will be used on metrics that are captured on a per-graph basis.

4.6.1 Friedman Test

We will be testing the statistical significance of the differences in metrics calculated from the graphs of both subject pools. The Friedman test, similar to the parametric repeated measures ANOVA, is a non-parametric test used for one-way repeated measures of variance by ranks (Friedman, 1937). It tests the null hypothesis that two sets of measurements of the same individuals have the same distribution (Jones et al., 2001). We will be using the Friedman test on every average of every metric for each node to understand if there is a statistically significant difference in the information captured by that metric on the nodes or edges of the graphs of subjects with ASD and TD, with a set p-value of 0.05.

4.6.2 Wilcoxon Signed-Rank Test

The Wilcoxon signed-rank test is a non-parametric test used to compare two samples to test the null hypothesis that their population mean ranks differ. We'll be using it to compare the results of whole-graph measurements for all graphs in both samples, such as transitivity or global efficiency.

The principal reason why we are using the Wilcoxon signed-rank test rather than the pared Student's t-test is because it does not require us to assume that our distribution is normally distributed (Lowry, 2014), which is not an assumption, particularly with our relatively small number of examples, that we want to make. This makes the Wilcoxon signed-rank test a more reasonable method for our particular use. We will set our p-value to 0.05.

5 Initial Results

We have already run a majority of the metrics discussed previously on all of the graphs on both ASD and TD networks. The top five nodes and their corresponding average metric across all networks for each value are presented in Tables 2 and 1. Just a sampling of the top 5 nodes indicates that there seem to be some notable differences between the metrics on ASD and TD subjects, which is promising to our current research. We will proceed by calculating the p-score of these and the remaining metrics with the Friedman and Wilcoxon signed-rank tests in order to determine the statistical significance of these differences.

6 Further Work

Once we have all metrics calculated we will delve deeper into the graph aspects which presented greater statistical significance between the two groups – we will not know what these necessarily are until we have all of our results computer. Our ultimate goal is to tie this information back to the literature on autism detailed in the **Related Work** section and on the function of various brain regions to understand whether our findings and results align with current knowledge on white matter structure in individuals with ASD, or whether there are certain aspects of the structure that has not been captured by current knowledge and efforts in this field. Depending on the significance of these results, we are also planning on comparing both graphs to null models. We would be running configuration models for each of the networks, generating 1000 for each. These null models can ground our research and our understanding of the structure of white matter in the brain for both subject pools, as we can calculate the statistical significance in difference between metrics of both subject sets and the null model.

We hope that with the research performed for this project we will be able to gain greater and new insight as to the differences in structure and form of white matter in adolescents and preteens.

References

UCSD Autism Center of Excellence ACE. 2016. Diffusion tensor imaging (dti).

Sophie Achard and Ed Bullmore. 2007. Efficiency and cost of economical brain functional networks. *PLoS Comput Biol*, 3(2):e17.

Naama Barnea-Goraly, Hower Kwon, Vinod Menon, Stephan Eliez, Linda Lotspeich, and Allan L Reiss. 2004. White matter structure in autism: preliminary evidence from diffusion tensor imaging. *Biological psychiatry*, 55(3):323–326.

Ulrik Brandes. 2001. A faster algorithm for betweenness centrality*. *Journal of mathematical sociology*, 25(2):163–177.

Jesse A Brown, Jeffrey D Rudie, Anita Bandrowski, John D Van Horn, and Susan Y Bookheimer. 2012. The ucla multimodal connectivity database: a web-based platform for brain connectivity matrix sharing and analysis. *Frontiers in neuroinformatics*, 6:28.

Adriana Di Martino, Chao-Gan Yan, Qingyang Li, Erin Denio, Francisco X Castellanos, Kaat Alaerts, Jeffrey S Anderson, Michal Assaf, Susan Y Bookheimer, Mirella Dapretto, et al. 2014. The autism brain imaging data exchange: towards a large-scale evaluation of the intrinsic brain architecture in autism. *Molecular psychiatry*, 19(6):659–667.

R Douglas Fields. 2008. White matter matters. *Scientific American*, 298(3):54–61.

Milton Friedman. 1937. The use of ranks to avoid the assumption of normality implicit in the analysis of variance. *Journal of the american statistical association*, 32(200):675–701.

Eric Jones, Travis Oliphant, Pearu Peterson, et al. 2001–. SciPy: Open source scientific tools for Python.

Karen E Joyce, Paul J Laurienti, Jonathan H Burdette, and Satoru Hayasaka. 2010. A new measure of centrality for brain networks. *PLoS One*, 5(8):e12200.

Timothy A Keller, Rajesh K Kana, and Marcel Adam Just. 2007. A developmental study of the structural integrity of white matter in autism. *Neuroreport*, 18(1):23–27.

Jon M Kleinberg. 1999. Authoritative sources in a hyperlinked environment. *Journal of the ACM (JACM)*, 46(5):604–632.

Amy N Langville and Carl D Meyer. 2005. A survey of eigenvector methods for web information retrieval. *SIAM review*, 47(1):135–161.

Gabriele Lohmann, Daniel S Margulies, Annette Horstmann, Burkhard Pleger, Joeran Lepsien, Dirk Goldhahn, Haiko Schloegl, Michael Stumvoll, Arno Villringer, and Robert Turner. 2010. Eigenvector centrality mapping for analyzing connectivity patterns in fmri data of the human brain. *PloS one*, 5(4):e10232.

Catherine Lord, Edwin H Cook, Bennett L Leventhal, and David G Amaral. 2000. Autism spectrum disorders. *Neuron*, 28(2):355–363.

Richard Lowry. 2014. Concepts and applications of inferential statistics.

PM Matthews and P Jezzard. 2004. Functional magnetic resonance imaging. *Journal of Neurology, Neurosurgery & Psychiatry*, 75(1):6–12.

Susumu Mori and Peter van Zijl. 2002. Fiber tracking: principles and strategies–a technical review. *NMR in Biomedicine*, 15(7-8):468–480.

National Institute of Mental Health NIMH. 2016. Autism spectrum disorder.

Tore Opsahl, Filip Agneessens, and John Skvoretz. 2010. Node centrality in weighted networks: Generalizing degree and shortest paths. *Social networks*, 32(3):245–251.

Lawrence Page, Sergey Brin, Rajeev Motwani, and Terry Winograd. 1999. The pagerank citation ranking: bringing order to the web.

Jonathan D Power, Alexander L Cohen, Steven M Nelson, Gagan S Wig, Kelly Anne Barnes, Jessica A Church, Alecia C Vogel, Timothy O Laumann, Fran M Miezin, Bradley L Schlaggar, et al. 2011. Functional network organization of the human brain. *Neuron*, 72(4):665–678.

Jennifer R Pryweller, Kimberly B Schauder, Adam W Anderson, Jessica L Heacock, Jennifer H Foss-Feig, Cassandra R Newsom, Whitney A Loring, and Carissa J Cascio. 2014. White matter correlates of sensory processing in autism spectrum disorders. *NeuroImage: Clinical*, 6:379–387.

Mikail Rubinov and Olaf Sporns. 2010. Complex network measures of brain connectivity: uses and interpretations. *Neuroimage*, 52(3):1059–1069.

Jeffrey D Rudie, JA Brown, D Beck-Pancer, LM Hernandez, EL Dennis, PM Thompson, SY Bookheimer, and M Dapretto. 2013. Altered functional and structural brain network organization in autism. *NeuroImage: clinical*, 2:79–94.

Olaf Sporns, Christopher J Honey, and Rolf Kötter. 2007. Identification and classification of hubs in brain networks. *PloS one*, 2(10):e1049.

Andrew Zalesky, Alex Fornito, Ian H Harding, Luca Cocchi, Murat Yücel, Christos Pantelis, and Edward T Bullmore. 2010. Whole-brain anatomical networks: does the choice of nodes matter? *Neuroimage*, 50(3):970–983.